

Explicit analytical solutions for two-dimensional contact detection problems between almost arbitrary geometries and straight or circular counterparts

Ulrich J. Römer^{a,*}, Alexander Fidlin^a, Wolfgang Seemann^a

^a*Institute of Engineering Mechanics, Karlsruhe Institute of Technology, Kaiserstraße 10, 76131 Karlsruhe, Germany*

Abstract

Contact between complex bodies and simple counterparts like straight lines or circles occur in many two-dimensional mechanical models. The corresponding contact detection problems are complicated and thus far, no explicit formulas have been available. In this paper, we address the contact detection problem between two planar bodies: one being either a straight line or a circle and the other an almost arbitrary geometry — the only requirement is a unique contact point for all possible contact situations. To solve this general problem, a novel procedure is applied which provides necessary conditions for the description of the geometry based on the special case of a rolling contact. This results in a parameterization of the geometry which gives the potential contact point depending on the relative orientation between the two bodies. Although the derivation is based on a rolling contact, the result is valid in general and can also be used for efficient contact detection when the bodies are separated. The derived equations are simple and easy to implement, which is demonstrated for two examples: a foot-ground contact model and a cam-follower mechanism.

Keywords: Contact detection, Contact kinematics, Two-dimensional contact, Analytical solution, Cam-follower mechanism, Foot-ground contact

1. Introduction

Contact problems occur frequently in many mechanical models. However, there are almost no explicit analytical solutions to calculate (potential) contact points directly except for combinations of simple geometric primitives, e.g. point-plane, point-sphere, sphere-sphere, plane-sphere, plane-ellipsoid and plane-superellipsoid [1, 2]. An analytical solution for the contact between two hard ellipses was published as late as 2007 [3] while the three-dimensional contact between two ellipsoids is yet to be solved analytically. Therefore, solutions of the contact detection problem usually rely on numerical methods [4] even if the counterparts are ellipsoids [5], superellipsoids [1], or more general quadric and superquadric surfaces [6] and even superovoids [7]. Due to the iterative nature of the numerical approaches they are computationally more expensive and time consuming than explicit solutions. Furthermore, the dynamics of such systems cannot be formulated in a set of minimal coordinates because the implicit constraint equations cannot be eliminated. The result is a set of differential algebraic equations for the system dynamics instead of an ordinary differential equation, which requires an appropriate technique for the numerical solution [8]. It is also very difficult, if not impossible, to investigate these models analytically.

The basic definition of the potential contact point on two lines or surfaces follows from the normal vectors, also known as common normal concept. If both counterparts are regular, which means the curvature is well-defined and non-singular, the normal vectors in both potential contact points are anti-parallel. Numerical methods in literature predominantly use one of the following three approaches: one approach is to calculate these points iteratively [1, 6, 9]. Another approach is to distribute a finite number of points on every surface and solve the combinatorial problem of which points are the closest ones [4, 10]. The gaps between the points are interpolated to detect contacts and

*Corresponding author

Email addresses: ulrich.roemer@kit.edu (Ulrich J. Römer), alexander.fidlin@kit.edu (Alexander Fidlin), wolfgang.seemann@kit.edu (Wolfgang Seemann)

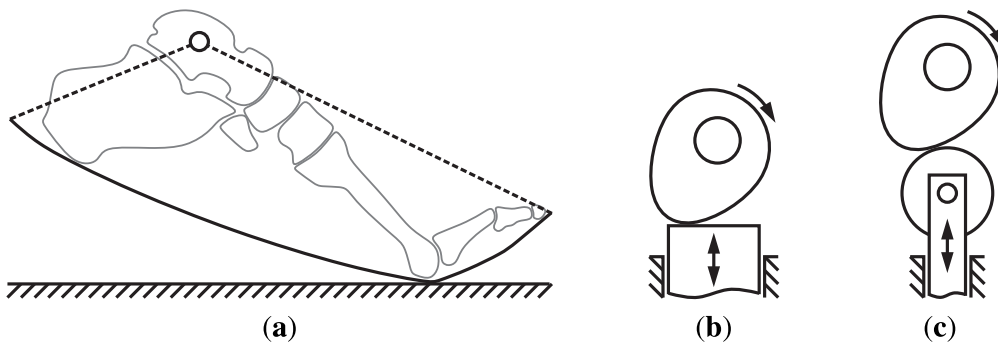


Figure 1: (a) Rolling contact of rigid foot model on flat ground, (b) sliding contact of camshaft and bucket tappet, and (c) rolling/sliding contact of camshaft and roller tappet

penetration. A different approach can be used if one of the contacting bodies has a simple geometry. For instance in cam-follower mechanisms, the counterpart of the cam is often a circle. The constant radius of the circle means that its center is equidistant from the cam. Thus, this special contact problem can be solved by calculating an equidistant curve, which is possible for parameterizations via pythagorean-hodograph curves [11].

There is a variety of contact problems where only one of the involved bodies has a complex shape and the counterpart is a plane or cylinder – a straight line or circle when projected onto two dimensions. Some examples are the foot-ground interaction model in Fig. 1a with applications in biomechanics and kinesiology, the sliding contact between a cam and a bucket tappet in Fig. 1b, and the rolling contact between a cam and a roller tappet in Fig. 1c. The latter two examples are models for cam-follower mechanisms which are frequently used to control the valves in internal combustion engines.

In this paper, explicit solutions for the two-dimensional contact detection problem between a body with complex shape and a straight line or a circle are derived which require only uniqueness of the (potential) contact point and piecewise differentiability of the body's boundary. In the case of a circular counterpart, uniqueness of the contact point means that the geometry of the body under consideration does not have to be strictly convex (or strictly concave). Rather, the body's boundary may consist of convex and concave sections, as long as the assumption of the uniqueness of the contact point is not violated. A shape whose boundary consists mainly of convex (concave) sections and which meets this condition is hereinafter referred to as *almost convex (almost concave)*, whereby strictly convex (strictly concave) shapes are also included in this definition.

The paper is organized as follows. The contact between a circular wheel and a straight line is reviewed in Sect. 2. This highlights the advantage of an explicit analytical solution of the contact kinematics for the special case of rolling constraints and its consequences for the formulation of the system's dynamics. The consideration of rolling constraints introduces necessary conditions for the position of the contact point. This approach is first motivated with the contact between an ellipse and a straight line in Sect. 3. It is then generalized further for contacts between arbitrary convex shapes and a straight line in Sect. 4 and finally for almost convex and almost concave shapes and a circle in Sect. 5. The resulting contact detection approach is applied to two examples in Sect. 6. A generic model of a rolling foot is treated in Sect. 6.1, and the contact of camshaft and roller tappet in Sect. 6.2. Finally, the described approach for explicit solutions of planar contact detection problems with straight or circular counterparts is briefly summarized and a proposition for future work is given in Sect. 7.

2. Contact between a circular wheel and a straight line

The circular wheel rolling on flat ground in Fig. 2a is a textbook example for a constrained rigid body motion which can be described by minimal coordinates. This problem is often discussed in introductory lectures on mechanics due to its simplicity. The aim is to derive the equation of motion using the angle as coordinate. However, since the problem is so simple, conceptually important steps in the solution are often not written out explicitly because they are trivial in case of the circular wheel. Therefore, it is difficult to apply this procedure to other geometries where the calculation of the contact point in particular is considerably more complicated. Before the general contact between a

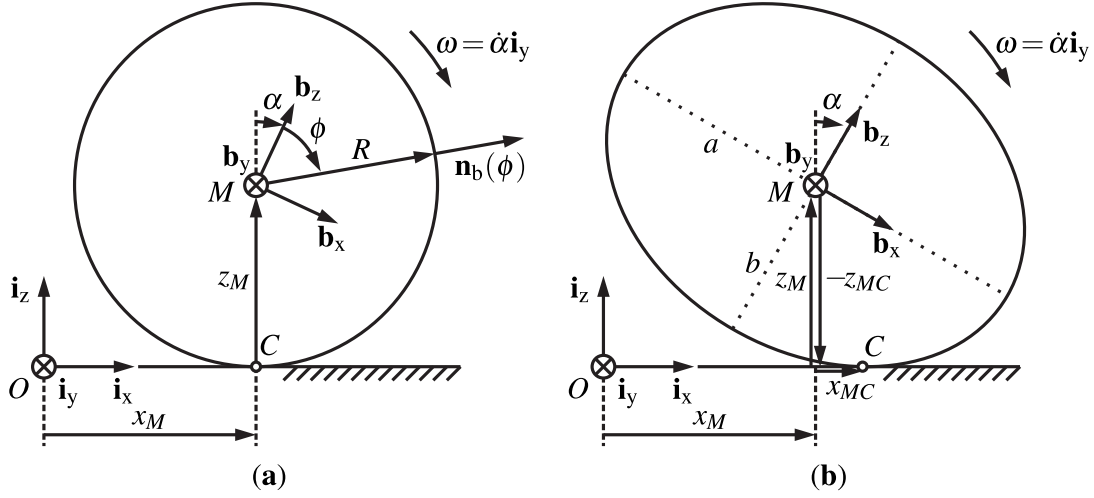


Figure 2: Contact between a straight line and (a) a circular wheel, and (b) an ellipse

complex geometry and a straight line is addressed in the following sections, two different perspectives on this problem are discussed using this simple example: the geometrical perspective in which the contact point is derived from the common normal concept, and the mechanical perspective in which the contact point is the wheel's instantaneous center of rotation due to the rolling constraints. Usually these two steps — determination of the contact point with the common normal concept and introduction of constraints at the contact point in order to restrict the movement — are executed in this order. Before we use the example of a rolling ellipse in the next section to demonstrate that this sequence is not absolutely necessary and that the mechanical approach provides useful geometric relationships, the standard procedure is discussed using the rolling wheel.

The three generalized coordinates of the unconstrained body must satisfy two (holonomic) constraint equations which can be formulated explicitly, thus allowing for a reduction to one minimal coordinate. Without loss of generality let the straight line be fixed in the inertial frame \mathcal{I} with the origin O somewhere on the line. The tangential and normal vectors of the line are \mathbf{i}_x and \mathbf{i}_z , respectively. A body-fixed reference frame \mathcal{B} with $\mathbf{b}_y = \mathbf{i}_y$ is attached to the wheel with center M and radius R . The position and orientation of the unconstrained wheel in the $\{\mathbf{i}_x, \mathbf{i}_z\}$ -plane is described by the three generalized coordinates $\mathbf{q} = [x_M(t), z_M(t), \alpha(t)]^T$. For the sake of clarity, the explicit time dependency of all variables is dropped below. The position of the wheel's center is

$$\mathbf{r}_M = x_M \mathbf{i}_x + z_M \mathbf{i}_z \quad (1)$$

and its angular velocity $\omega = \dot{\alpha} \mathbf{i}_y$ (time derivatives are denoted by a dot) is positive in clockwise direction. The outer normal vector of any point given by the angle ϕ on the wheel's boundary is $\mathbf{n}_b(\phi) = \sin(\phi + \alpha) \mathbf{i}_x + \cos(\phi + \alpha) \mathbf{i}_z$. There is one point C on the wheel's boundary where the normal vector $\mathbf{n}_b(\phi_C)$ is anti-parallel to the normal vector $\mathbf{n}_l = \mathbf{i}_z$ of the line. C is the potential contact point¹ which is defined by the implicit equation

$$\mathbf{n}_b(\phi_C) \cdot \mathbf{n}_l = -1 \quad (2)$$

which yields

$$\begin{aligned} \cos(\phi_C + \alpha) &= -1, \\ \phi_C &= \pi - \alpha \end{aligned} \quad (3)$$

¹The potential contact point is defined as the point on the boundary which is in contact with the body's counterpart when there is no gap. If the counterpart is a straight line it is also the point which is the closest to the line when there is a gap. However, this is not the case if the counterpart's curvature is non-zero, cf. Sect. 5.

for the circle. Therefore, the position of C is

$$\begin{aligned}\mathbf{r}_{MC} &= R \sin(\phi_C + \alpha) \mathbf{i}_x + R \cos(\phi_C + \alpha) \mathbf{i}_z \\ &= -R \mathbf{i}_z,\end{aligned}\tag{4a}$$

$$\begin{aligned}\mathbf{r}_C &= \mathbf{r}_M + \mathbf{r}_{MC} \\ &= x_M \mathbf{i}_x + (z_M - R) \mathbf{i}_z\end{aligned}\tag{4b}$$

and its velocity is

$$\begin{aligned}\dot{\mathbf{r}}_C = \mathbf{v}_C &= \mathbf{v}_M + \boldsymbol{\omega} \times \mathbf{r}_{MC} \\ &= (\dot{x}_M - R\dot{\alpha}) \mathbf{i}_x + \dot{z}_M \mathbf{i}_z.\end{aligned}\tag{4c}$$

Contact of the wheel and the line arises from the normal constraint

$$\begin{aligned}\mathbf{r}_C \cdot \mathbf{i}_z &= z_M - R = 0 \\ \Rightarrow z_M(t) &= R, \quad \dot{z}_M(t) = 0, \quad \ddot{z}_M(t) = 0\end{aligned}\tag{5}$$

and rolling from the tangential constraint

$$\mathbf{v}_C \cdot \mathbf{i}_x = \dot{x}_M - R\dot{\alpha} = 0.\tag{6}$$

This holonomic constraint can be integrated yielding

$$x_M(t) = R\alpha(t) + x_{M,0}\tag{7}$$

with the constant $x_{M,0}$. The constrained problem can thus be expressed by one minimal coordinate, e.g. $\alpha(t)$ or $x_M(t)$.

It is important to recall that this is only possible because there is an explicit solution for Eq. (2) which defines the contact point on the wheel's boundary and on the line. If the rolling condition holds, the velocity $\mathbf{v}_C = 0$ and the contact point C is the wheel's instantaneous center of rotation. The explicit solution Eq. (4a) for the kinematics of point C is also useful if the interaction between the wheel and the line is assumed to be elastic and the interaction is defined by a different contact force law² like a normal stiffness from the Hertz model [13] and any friction law in tangential direction [4, 9].

Explicit solutions of Eq. (2) exist only for the contact between special shapes, cf. Sect. 1. In general, Eq. (2) has to be solved numerically. However, the considerations above show that the specification of Eqs. (4a) and (5) – the position of the potential contact point relative to the wheel's center – gives a complete parameterization of the circular boundary and allows for the explicit solution of the constraint equations. The parameterization of the potential contact point for a certain counterpart is not restricted to the circular wheel but applicable to many shapes. As first step in the generalization of this concept, the contact between an ellipse and a straight line is treated in the next section.

3. Contact between an ellipse and a straight line

The contact between an ellipse and a straight line which is displayed in Fig. 2b is similar to the example of the rolling circular wheel but with a non-constant distance between the center and the boundary. Without loss of generality let again the straight line be fixed in the inertial frame \mathcal{I} with the origin O somewhere on the line. The tangential and normal vectors of the line are \mathbf{i}_x and \mathbf{i}_z , respectively. A body-fixed reference frame \mathcal{B} with $\mathbf{b}_y = \mathbf{i}_y$ is attached to the ellipse's center M such that the semiaxes a and b are in the directions \mathbf{b}_x and \mathbf{b}_z , respectively.

²A widespread approach in multibody simulations is to weaken the assumption of rigidity and allow for small penetrations of two contacting bodies. The perceived penetrations result in deformations of both bodies in a small neighborhood of C which are then described via half space models, assuming the contact area is much smaller than the bodies' dimensions. The contact forces at C follow from the integration of the respective pressure over the contact area and act like nonlinear spring-damper-elements, cf. [12].

The position and orientation of the unconstrained ellipse in the $\{\mathbf{i}_x, \mathbf{i}_z\}$ -plane is described by the three generalized coordinates $\mathbf{q} = [x_M(t), z_M(t), \alpha(t)]^T$. A calculation of the potential contact point

$$\mathbf{r}_{MC} = x_{MC} \mathbf{i}_x + z_{MC} \mathbf{i}_z \quad (8)$$

analogously to Eqs. (1) – (3) yields

$$z_{MC}(\alpha) = -\sqrt{b^2 \cos^2(\alpha) + a^2 \sin^2(\alpha)}, \quad (9)$$

which only depends on the ellipse's orientation relative to the straight line. For the special case $R = a = b$ this is equal to Eq. (4) for the circular wheel.

The distance x_{MC} can either be obtained by geometrical considerations which make use of relationships which are unique for the ellipse, or from the observation in the previous example, that the contact point becomes the instantaneous center of rotation if the normal and tangential constraints for rolling are imposed. The position and velocity of C are

$$\begin{aligned} \mathbf{r}_C &= \mathbf{r}_M + \mathbf{r}_{MC} \\ &= (x_M + x_{MC}) \mathbf{i}_x + \left(z_M - \sqrt{b^2 \cos^2(\alpha) + a^2 \sin^2(\alpha)} \right) \mathbf{i}_z, \end{aligned} \quad (10a)$$

$$\begin{aligned} \mathbf{v}_C &= \mathbf{v}_M + \boldsymbol{\omega} \times \mathbf{r}_{MC} \\ &= \left(\dot{x}_M - \dot{\alpha} \sqrt{b^2 \cos^2(\alpha) + a^2 \sin^2(\alpha)} \right) \mathbf{i}_x + (\dot{z}_M - x_{MC} \dot{\alpha}) \mathbf{i}_z \end{aligned} \quad (10b)$$

and the rolling constraints yield

$$z_M = \sqrt{b^2 \cos^2(\alpha) + a^2 \sin^2(\alpha)}, \quad (11a)$$

$$\dot{z}_M = x_{MC}(\alpha) \dot{\alpha}. \quad (11b)$$

The last equation can be simplified using chain rule

$$\dot{z}_M = z'_M(\alpha) \dot{\alpha} = x_{MC}(\alpha) \dot{\alpha} \quad (12)$$

(derivatives with respect to a function's argument are denoted by prime) which yields the relationship

$$x_{MC}(\alpha) = z'_M(\alpha) = \frac{(a^2 - b^2) \sin(2\alpha)}{2 \sqrt{b^2 \cos^2(\alpha) + a^2 \sin^2(\alpha)}}. \quad (13)$$

Therefore, Eq. (9) gives a complete parameterization of the ellipse because x_{MC} follows directly from Eq. (13). However, this relationship is not limited to circles and ellipses. The considerations above can be generalized to arbitrary shapes as long as the contact point is unique for all angles α . The special case of rolling is used to derive consistency conditions for the position of the potential contact point on the bodies boundary. A generalization for the contact detection problem between arbitrary convex bodies and straight lines is given in the next section.

4. Contact between a convex body and a straight line

The contact problem of an arbitrary convex body with a straight line is depicted in Fig. 3a. Example models of applications with this kind of contact are the foot model on flat ground in Fig. 1a and the cam-follower mechanism in Fig. 1b.

Let the line again be fixed in the inertial frame \mathcal{I} with the origin O somewhere on the line. The tangential and normal vectors of the line are \mathbf{i}_x and \mathbf{i}_z , respectively. A body-fixed reference frame \mathcal{B} with $\mathbf{b}_y = \mathbf{i}_y$ is attached to the convex body at some point P . The body's three degrees of freedom are described by the generalized coordinates

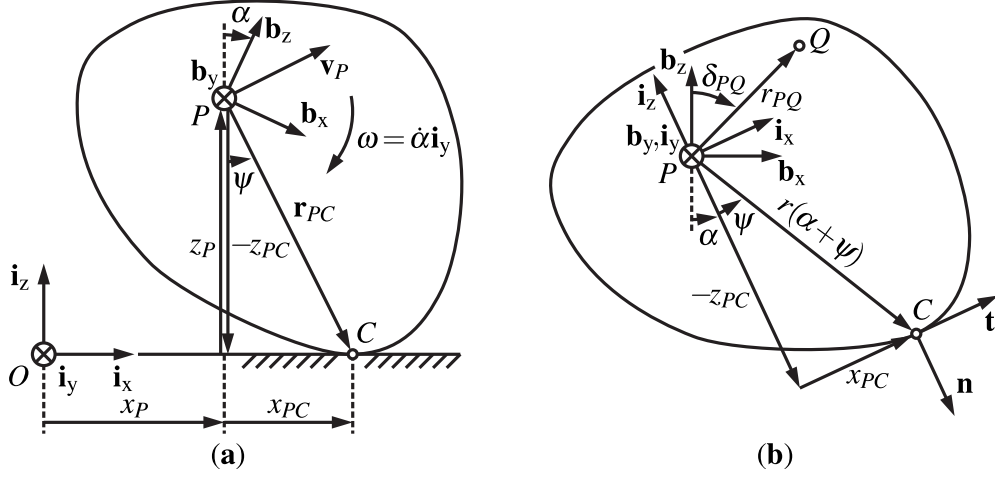


Figure 3: (a) Contact between a convex body and a straight line (observed in the inertial frame T), and (b) parameterization of its boundary in polar coordinates (observed in the body-fixed frame B)

$\mathbf{q} = [x_P(t), z_P(t), \alpha(t)]^T$. As observed in the previous example and the depiction in Fig. 3a, the position of the potential contact point C relative to P depends only on the orientation α . Assuming that C is unique for all α , this relative position $\mathbf{r}_{PC}(\alpha)$ follows from a scalar function $f_P : \mathbb{S} \rightarrow \mathbb{R}$, $f_P \in C^2$. The function $f_P(\alpha)$ is a parameterization of the minimal distance between P and the line – the projection of the vector from P to C onto the line's normal \mathbf{i}_z (cf. Eq. (19)). Its specific form depends on the shape of the body's boundary which must be 2π -periodic with respect to α . C being unique means that there are no straight line segments of the boundary meaning its curvature is non-zero everywhere.

The dependency of $\mathbf{r}_{PC}(\alpha)$ on $f_P(\alpha)$ can be derived considering the special case of a rolling contact between the body and the plane. The system is then reduced to one degree of freedom and the positions of P and C become functions of the angle

$$\mathbf{r}_P = x_P(\alpha) \mathbf{i}_x + z_P(\alpha) \mathbf{i}_z, \quad (14)$$

$$\mathbf{r}_C = x_C(\alpha) \mathbf{i}_x, \quad (15)$$

$$\begin{aligned} \mathbf{r}_{PC} &= \mathbf{r}_C - \mathbf{r}_P \\ &= x_{PC}(\alpha) \mathbf{i}_x + z_{PC}(\alpha) \mathbf{i}_z, \end{aligned} \quad (16)$$

and thus

$$z_P(\alpha) = -z_{PC}(\alpha). \quad (17)$$

The definition of

$$z_P(\alpha) = f_P(\alpha) \quad (18)$$

for this case thus also yields

$$z_{PC}(\alpha) = -f_P(\alpha). \quad (19)$$

The dependency of $x_{PC}(\alpha)$ on $f_P(\alpha)$ follows from the velocity of P for an arbitrary angular velocity $\boldsymbol{\omega} = \dot{\alpha} \mathbf{i}_y$ which can be derived in two ways: differentiation of the position yields

$$\begin{aligned} \dot{\mathbf{r}}_P &= \mathbf{v}_P = \dot{x}_P(\alpha) \mathbf{i}_x + \dot{z}_P(\alpha) \mathbf{i}_z \\ &= x'_P(\alpha) \dot{\alpha} \mathbf{i}_x + z'_P(\alpha) \dot{\alpha} \mathbf{i}_z \\ &= x'_P(\alpha) \dot{\alpha} \mathbf{i}_x + f'_P(\alpha) \dot{\alpha} \mathbf{i}_z, \end{aligned} \quad (20)$$

and the rolling condition

$$\dot{\mathbf{r}}_C = \mathbf{v}_C = \mathbf{0} \quad (21)$$

results in

$$\begin{aligned} \mathbf{v}_P &= \mathbf{v}_C + \boldsymbol{\omega} \times \mathbf{r}_{CP} \\ &= \mathbf{0} + \mathbf{r}_{PC} \times \boldsymbol{\omega} \\ &= -z_{PC}(\alpha)\dot{\alpha} \mathbf{i}_x + x_{PC}(\alpha)\dot{\alpha} \mathbf{i}_z \\ &= f_P(\alpha)\dot{\alpha} \mathbf{i}_x + x_{PC}(\alpha)\dot{\alpha} \mathbf{i}_z . \end{aligned} \quad (22)$$

Comparison of the coefficients in Eqs. (20) and (22) yields

$$x_{PC}(\alpha) = f'_P(\alpha) , \quad (23)$$

$$x_P(\alpha) = x_{P,0} + \int_0^\alpha f_P(\bar{\alpha}) d\bar{\alpha} , \quad (24)$$

$$x_C(\alpha) = x_{P,0} + \int_0^\alpha f_P(\bar{\alpha}) d\bar{\alpha} + f'_P(\alpha) . \quad (25)$$

Therefore, the relative position of the potential contact point is

$$\mathbf{r}_{PC}(\alpha) = f'_P(\alpha) \mathbf{i}_x - f_P(\alpha) \mathbf{i}_z \quad (26)$$

and an implicit definition of the boundary in polar coordinates r and φ

$$\|\mathbf{r}_{PC}(\alpha)\|_2 = r(\alpha) = \sqrt{f'_P(\alpha)^2 + f_P(\alpha)^2} , \quad (27)$$

$$\psi(\alpha) = \arctan\left(\frac{f'_P(\alpha)}{f_P(\alpha)}\right) , \quad (28)$$

$$\alpha + \psi(\alpha) = \varphi(\alpha) = \alpha + \arctan\left(\frac{f'_P(\alpha)}{f_P(\alpha)}\right) \quad (29)$$

follows from Fig. 3b. The continuity of this parameterization of the geometry via $\mathbf{r}_{PC}(\alpha)$ depends on the definition of $f'_P(\alpha)$. If $f'_P(\alpha) \in C^k$ then $\mathbf{r}_{PC}(\alpha) \in C^{k-1}$ which means a continuous boundary requires $k \geq 1$. The curvature of the boundary at the current point $C(\alpha)$ can be derived as follows: the position of C in \mathcal{B} is

$$\mathbf{r}_{PC} = f'_P(\alpha) \mathbf{i}_x(\alpha) - f_P(\alpha) \mathbf{i}_z(\alpha) \quad (30)$$

with

$$\mathbf{i}_x(\alpha) = \cos(\alpha) \mathbf{b}_x + \sin(\alpha) \mathbf{b}_z , \quad (31a)$$

$$\mathbf{i}_y(\alpha) = \mathbf{b}_y , \quad (31b)$$

$$\mathbf{i}_z(\alpha) = -\sin(\alpha) \mathbf{b}_x + \cos(\alpha) \mathbf{b}_z . \quad (31c)$$

The tangent and normal vectors are

$$\mathbf{t}(\alpha) = \mathbf{i}_x(\alpha) , \quad (32a)$$

$$\mathbf{n}(\alpha) = \mathbf{i}_z(\alpha) \quad (32b)$$

with the derivatives

$$\frac{d}{d\alpha} \mathbf{t}(\alpha) = \mathbf{i}_z(\alpha) = \mathbf{n}(\alpha) , \quad (33a)$$

$$\frac{d}{d\alpha} \mathbf{n}(\alpha) = -\mathbf{i}_x(\alpha) = -\mathbf{t}(\alpha) , \quad (33b)$$

and the curvature $\kappa(\alpha)$ follows from the differentiation of the tangent vector \mathbf{t} with respect to the arclength s

$$\frac{d}{ds}\mathbf{t}(\alpha) = \frac{d}{d\alpha}\mathbf{t}(\alpha)\frac{d\alpha}{ds} = \kappa(\alpha)\mathbf{n}(\alpha), \quad (34)$$

$$\Rightarrow \kappa(\alpha) = \frac{d\alpha}{ds} = \left(\frac{ds}{d\alpha}\right)^{-1}. \quad (35)$$

Due to the rolling condition, the arclength on the body's boundary between two points $C(\alpha_1)$ and $C(\alpha_2)$ is equal to the length of the line segment between the two corresponding points. Therefore, the derivative of the arclength s with respect to α follows from the derivative of the position of C in the inertial frame \mathcal{I}

$$\frac{ds}{d\alpha} = \frac{d}{d\alpha}x_C(\alpha) = f_P''(\alpha) + f_P(\alpha). \quad (36)$$

The curvature is thus

$$\kappa(\alpha) = (f_P''(\alpha) + f_P(\alpha))^{-1}. \quad (37)$$

A necessary restriction for admissible functions $f_P(\alpha)$ is $\kappa(\alpha) > 0, \forall \alpha$ as assumed above. As for the examples of the rolling circular wheel and the ellipse, it is important to stress that the relationship Eq. (30) holds also when there is no rolling, or even no contact between the body and the line.

Although the condition of positive curvature on the body's boundary results in uniqueness of C , the parameterization of the boundary itself is not unique. In fact, there are infinitely many parameterizations of the same boundary which differ only in their respective body-fixed reference point. The transformation of the parameterization from the reference point P to the reference point Q is straightforward, cf. Fig. 3b. The kinematics of Q relative to P are

$$\begin{aligned} \mathbf{r}_{PQ} &= x_{PQ}(\alpha)\mathbf{i}_x + z_{PQ}(\alpha)\mathbf{i}_z \\ &= r_{PQ}\sin(\alpha + \delta_{PQ})\mathbf{i}_x + r_{PQ}\cos(\alpha + \delta_{PQ})\mathbf{i}_z, \end{aligned} \quad (38)$$

the absolute position is

$$\begin{aligned} \mathbf{r}_Q &= \mathbf{r}_P + \mathbf{r}_{PQ} \\ &= x_Q(\alpha)\mathbf{i}_x + z_Q(\alpha)\mathbf{i}_z \\ &= (x_P(\alpha) + r_{PQ}\sin(\alpha + \delta_{PQ}))\mathbf{i}_x + (z_P(\alpha) + r_{PQ}\cos(\alpha + \delta_{PQ}))\mathbf{i}_z, \end{aligned} \quad (39)$$

and the relative position of C is

$$\begin{aligned} \mathbf{r}_{QC} &= \mathbf{r}_{QP} + \mathbf{r}_{PC} = \mathbf{r}_{PC} - \mathbf{r}_{PQ} \\ &= x_{QC}(\alpha)\mathbf{i}_x + z_{QC}(\alpha)\mathbf{i}_z \\ &= (x_{PC}(\alpha) - r_{PQ}\sin(\alpha + \delta_{PQ}))\mathbf{i}_x + (z_{PC}(\alpha) - r_{PQ}\cos(\alpha + \delta_{PQ}))\mathbf{i}_z \\ &= (f_P'(\alpha) - r_{PQ}\sin(\alpha + \delta_{PQ}))\mathbf{i}_x - (f_P(\alpha) + r_{PQ}\cos(\alpha + \delta_{PQ}))\mathbf{i}_z. \end{aligned} \quad (40)$$

Therefore,

$$\begin{aligned} \mathbf{r}_C &= \mathbf{r}_P + \mathbf{r}_{PC} \\ &= \mathbf{r}_P + \mathbf{r}_{PQ} - \mathbf{r}_{PQ} + \mathbf{r}_{PC} \\ &= (\mathbf{r}_P + \mathbf{r}_{PQ}) + (\mathbf{r}_{PC} - \mathbf{r}_{PQ}) \\ &= \mathbf{r}_Q + \mathbf{r}_{QC}, \end{aligned} \quad (41)$$

which means the parameterization

$$f_Q(\alpha) = f_P(\alpha) + r_{PQ}\cos(\alpha + \delta_{PQ}) \quad (42)$$

results in the same contact point and boundary as before. This transformation is valid for any body-fixed point $Q \in \mathbb{R}^2$, not just for points inside the body's boundary.

5. Contact between a body and a circle

The contact between a body and a straight line from Sect. 4 can be generalized further to the contact between a body and a circle. The procedure is the same as in the previous section, albeit more complex because the orientation of the circle's outer normal vector is not constant in the inertial frame. Furthermore, there are two contact scenarios which are displayed in Figs. 4a and 4b, and referred to as *almost convex* and *almost concave*, respectively. As discussed in Sect. 1, the body's boundary may consist of convex and concave sections, as long as the assumption of the uniqueness of the contact point is not violated. Therefore, the term almost convex (almost concave) refers to a geometry which consists mainly of convex (concave) sections, whereby strictly convex (strictly concave) shapes are also included in this definition. Both scenarios follow from the same initial approach and the distinction of two cases for the solution of a quadratic equation.

Let the circle with radius R be fixed in the inertial frame \mathcal{I} with the origin O at its center. A body-fixed reference frame \mathcal{B} with $\mathbf{b}_y = \mathbf{i}_y$ is attached to the contacting body at point P . A moving reference frame \mathcal{K} with $\mathbf{k}_y = \mathbf{i}_y$ and origin O is introduced so that \mathbf{k}_z is always pointing from O to P . The rotation of \mathcal{K} relative to \mathcal{I} around \mathbf{i}_y is described by the angle ϕ . As is evident from Fig. 4, the position of the potential contact point C relative to P depends only on its orientation relative to \mathcal{K} which is described by the angle α . Furthermore, if there is contact between the body and the circle, the distance from the body's boundary to the circle's center O is equal to the radius R ; the point O is then in contact with a curve which is equidistant to the boundary. In the same way as in the previous section, the relative position of the potential contact point $\mathbf{r}_{R,PC}(\alpha)$ follows from a scalar function $g_{R,P} : \mathbb{S} \rightarrow \mathbb{R}$, $g_{R,P} \in C^2$ where the subscript R is shorthand for $\mathbf{r}_{R,PC}(\alpha) = \mathbf{r}_{PC}(\alpha, R)$ and $g_{R,P}(\alpha) = g_P(\alpha, R)$. The function $g_{R,P}(\alpha)$ is a parameterization of the equidistant curve with distance R from the body's boundary. If there is contact, this is equal to the distance between O and P (cf. Eq. (48)) which depends on the shape of the body's boundary and has to be 2π -periodic with respect to α . It is again assumed that C is unique for all α which is discussed below (cf. Eq. (72)).

The dependency of $\mathbf{r}_{PC}(\alpha)$ on $f_P(\alpha)$ follows again from the special case of rolling of the body on the circle. The system is then reduced to one degree of freedom and the positions of P and C become functions of the angle α

$$\mathbf{r}_{R,P} = z_{R,P}(\alpha) \mathbf{k}_z, \quad (43)$$

$$\mathbf{r}_{R,C} = x_{R,C}(\alpha) \mathbf{k}_x + z_{R,C}(\alpha) \mathbf{k}_z, \quad (44)$$

$$\begin{aligned} \mathbf{r}_{R,PC} &= \mathbf{r}_{R,C} - \mathbf{r}_{R,P} \\ &= x_{R,PC}(\alpha) \mathbf{k}_x + z_{R,PC}(\alpha) \mathbf{k}_z \end{aligned} \quad (45)$$

which yields

$$x_{R,C}(\alpha) = x_{R,PC}(\alpha), \quad (46)$$

$$\begin{aligned} z_{R,C}(\alpha) &= z_{R,P}(\alpha) + z_{R,PC}(\alpha) \\ &= \pm \sqrt{R^2 - x_{R,C}^2(\alpha)}. \end{aligned} \quad (47)$$

The two solutions of Eq. (47) correspond to the two different contact scenarios. Let

$$z_{R,P}(\alpha) = g_{R,P}(\alpha), \quad g_{R,P}(\alpha) > 0 \quad \forall \alpha \quad (48)$$

under the condition that the body is in contact with the circle. Due to the definition of reference frame \mathcal{K} , $g_{R,P}(\alpha)$ cannot be negative. The velocity of P for an arbitrary angular velocity $\boldsymbol{\omega}(\dot{\alpha}) = (\dot{\alpha} + \dot{\phi}(\alpha, \dot{\alpha})) \mathbf{k}_y$ is

$$\begin{aligned} \dot{\mathbf{r}}_{R,P} = \mathbf{v}_{R,P} &= z_{R,P}(\alpha) \dot{\phi}(\alpha, \dot{\alpha}) \mathbf{k}_x + \dot{z}_{R,P}(\alpha) \mathbf{k}_z \\ &= g_{R,P}(\alpha) \dot{\phi}(\alpha, \dot{\alpha}) \mathbf{k}_x + \dot{g}_{R,P}(\alpha) \mathbf{k}_z \\ &= g_{R,P}(\alpha) \dot{\phi}(\alpha, \dot{\alpha}) \mathbf{k}_x + g'_{R,P}(\alpha) \dot{\alpha} \mathbf{k}_z, \end{aligned} \quad (49)$$

and, with the rolling condition

$$\dot{\mathbf{r}}_{R,C} = \mathbf{v}_{R,C} = \mathbf{0}, \quad (50)$$

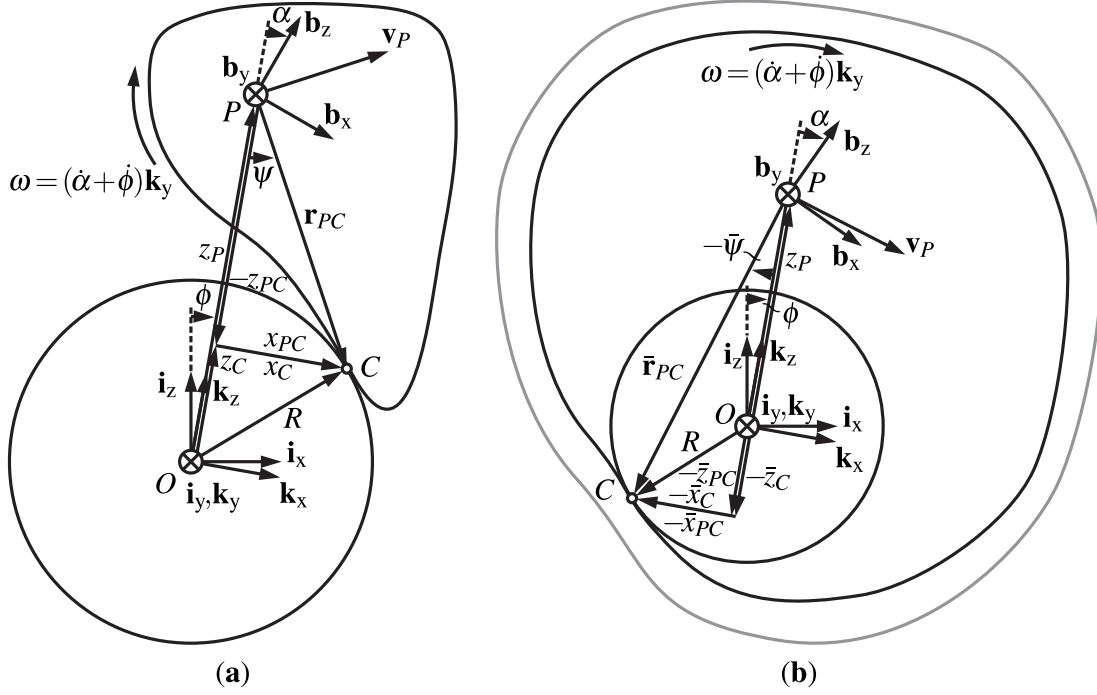


Figure 4: Contact between a circle and (a) an almost convex body, and (b) an almost concave body (observed in the inertial frame I)

also

$$\begin{aligned}
 \mathbf{v}_{R,P} &= \mathbf{v}_{R,C} + \omega(\alpha, \dot{\alpha}) \times \mathbf{r}_{R,CP}(\alpha) \\
 &= \mathbf{0} + \mathbf{r}_{R,PC}(\alpha) \times \omega(\alpha, \dot{\alpha}) \\
 &= -z_{R,PC}(\alpha) (\dot{\alpha} + \dot{\phi}(\alpha, \dot{\alpha})) \mathbf{k}_x + x_{R,PC}(\alpha) (\dot{\alpha} + \dot{\phi}(\alpha, \dot{\alpha})) \mathbf{k}_z.
 \end{aligned} \tag{51}$$

Equations (49) and (51) yield

$$\begin{aligned}
 \dot{\phi}(\alpha, \dot{\alpha}) &= -\frac{z_{R,PC}(\alpha)}{z_{R,P}(\alpha) + z_{R,PC}(\alpha)} \dot{\alpha} \\
 &= -\frac{z_{R,PC}(\alpha)}{z_{R,C}(\alpha)} \dot{\alpha}.
 \end{aligned} \tag{52}$$

Furthermore, because the velocity at C is zero it is the body's instantaneous center of rotation. Therefore, $\mathbf{r}_{R,PC}$ is perpendicular to the velocity vector in P : $\mathbf{r}_{R,PC} \cdot \mathbf{v}_{R,P} = 0$. Since the problem is two-dimensional, the direction of $\mathbf{r}_{R,PC}$ follows from $\mathbf{v}_{R,P}$ by interchanging of the \mathbf{k}_x - and the \mathbf{k}_z -components and negation of the \mathbf{k}_z -component. Division of both components by $\dot{\alpha}$ and scaling with $a(\alpha) \in \mathbb{R}$ yields

$$\mathbf{r}_{R,PC}(\alpha) = a(\alpha) g'_{R,P}(\alpha) \mathbf{k}_x - a(\alpha) \frac{g_{R,P}(\alpha) z_{R,PC}(\alpha)}{z_{R,C}(\alpha)} \mathbf{k}_z \tag{53}$$

and comparison with Eq. (45) results in

$$\frac{x_{R,PC}(\alpha)}{g'_{R,P}(\alpha)} = \frac{z_{R,C}(\alpha) z_{R,PC}(\alpha)}{g_{R,P}(\alpha) z_{R,PC}(\alpha)}. \tag{54}$$

Expressing $z_{R,C}(\alpha)$ via Eq. (47) and squaring both sides yields

$$x_{R,PC}^2(\alpha) g_{R,P}^2(\alpha) = (g'_{R,P}(\alpha))^2 (g_{R,P}(\alpha) + z_{R,PC}(\alpha))^2$$

which can be simplified further using $x_{R,PC}^2(\alpha) = (R^2 - (g_{R,P}(\alpha) + z_{R,PC}(\alpha))^2)$

$$(g_{R,P}(\alpha) + z_{R,PC}(\alpha))^2 = \frac{g_{R,P}^2(\alpha)}{g_{R,P}^2(\alpha) + (g'_{R,P}(\alpha))^2} R^2 .$$

This gives the solutions³

$$z_{R,PC}(\alpha) = -g_{R,P}(\alpha) + \frac{g_{R,P}(\alpha)}{\sqrt{g_{R,P}^2(\alpha) + g'_{R,P}{}^2(\alpha)}} R , \quad (55a)$$

$$x_{R,PC}(\alpha) = \frac{g'_{R,P}(\alpha)}{\sqrt{g_{R,P}^2(\alpha) + g'_{R,P}{}^2(\alpha)}} R = x_{R,C}(\alpha) , \quad (55b)$$

$$z_{R,C}(\alpha) = \frac{g_{R,P}(\alpha)}{\sqrt{g_{R,P}^2(\alpha) + g'_{R,P}{}^2(\alpha)}} R \quad (55c)$$

for the almost convex case (Fig. 4a) and

$$\bar{z}_{R,PC}(\alpha) = g_{R,P}(\alpha) + \frac{g_{R,P}(\alpha)}{\sqrt{g_{R,P}^2(\alpha) + g'_{R,P}{}^2(\alpha)}} R , \quad (56a)$$

$$\bar{x}_{R,PC}(\alpha) = -\frac{g'_{R,P}(\alpha)}{\sqrt{g_{R,P}^2(\alpha) + g'_{R,P}{}^2(\alpha)}} R = \bar{x}_{R,C}(\alpha) , \quad (56b)$$

$$\bar{z}_{R,C}(\alpha) = -\frac{g_{R,P}(\alpha)}{\sqrt{g_{R,P}^2(\alpha) + g'_{R,P}{}^2(\alpha)}} R \quad (56c)$$

for the almost concave case (Fig. 4b). Analogously to the result in Sect. 4, the continuity of this parameterization via $\mathbf{r}_{R,PC}(\alpha)$ depends on the definition of $g'_{R,P}(\alpha)$. If $g'_{R,P}(\alpha) \in C^k$ then $\mathbf{r}_{R,PC}(\alpha) \in C^{k-1}$ which means a continuous boundary requires $k \geq 1$. The restriction of the solution to either one case makes it unique. Indeed, for any shape with one contact point in the upper (lower) half circle with $z_{R,C}(\alpha) > 0$ ($\bar{z}_{R,C}(\alpha) < 0$) for any α , all contact points are on the upper (lower) half circle. To change from the upper (lower) half circle to the lower (upper) one, the point with $z_{R,C}(\alpha) = 0$ has to be passed which results in a singularity in Eq. (52)

$$\dot{\phi} = -\frac{z_{R,PC}(\alpha)}{z_{R,C}(\alpha)} \dot{\alpha} .$$

Because

$$g_{R,P}(\alpha) > 0 \quad \forall \alpha$$

via Eq. (48), this singularity cannot occur. As in Sect. 4, the body's boundary is implicitly defined in polar coordinates r, φ

$$\|\mathbf{r}_{R,PC}(\alpha)\|_2 = r(\alpha) = \sqrt{x_{R,PC}^2(\alpha) + z_{R,PC}^2(\alpha)} , \quad (57)$$

$$\psi(\alpha) = \arctan\left(\frac{x_{R,PC}(\alpha)}{-z_{R,PC}(\alpha)}\right) , \quad (58)$$

$$\alpha + \psi(\alpha) = \varphi(\alpha) = \alpha - \arctan\left(\frac{x_{R,PC}(\alpha)}{z_{R,PC}(\alpha)}\right) \quad (59)$$

³In Eqs. (55) – (73) all expressions which correspond to the almost concave case (Fig. 4b) are distinguished by a bar; expressions which correspond to the almost convex case (Fig. 4a) are without bar.

and $\bar{r}, \bar{\varphi}$

$$\|\bar{\mathbf{r}}_{R,PC}(\alpha)\|_2 = \bar{r}(\alpha) = \sqrt{\bar{x}_{R,PC}^2(\alpha) + \bar{z}_{R,PC}^2(\alpha)}, \quad (60)$$

$$\bar{\psi}(\alpha) = \arctan\left(\frac{\bar{x}_{R,PC}(\alpha)}{-\bar{z}_{R,PC}(\alpha)}\right), \quad (61)$$

$$\alpha + \bar{\psi}(\alpha) = \bar{\varphi}(\alpha) = \alpha - \arctan\left(\frac{\bar{x}_{R,PC}(\alpha)}{\bar{z}_{R,PC}(\alpha)}\right). \quad (62)$$

This parameterization of the boundary is depicted in Fig. 5 in the body-fixed reference frame \mathcal{B} . The boundary is given by

$$\mathbf{r}_{R,PC} = x_{R,PC}(\alpha) \mathbf{k}_x(\alpha) + z_{R,PC}(\alpha) \mathbf{k}_z(\alpha), \quad (63a)$$

$$\bar{\mathbf{r}}_{R,PC} = \bar{x}_{R,PC}(\alpha) \mathbf{k}_x(\alpha) + \bar{z}_{R,PC}(\alpha) \mathbf{k}_z(\alpha) \quad (63b)$$

in the reference frame

$$\mathbf{k}_x(\alpha) = \cos(\alpha) \mathbf{b}_x + \sin(\alpha) \mathbf{b}_z, \quad (64a)$$

$$\mathbf{k}_y(\alpha) = \mathbf{b}_y, \quad (64b)$$

$$\mathbf{k}_z(\alpha) = -\sin(\alpha) \mathbf{b}_x + \cos(\alpha) \mathbf{b}_z. \quad (64c)$$

with

$$\frac{d}{d\alpha} \mathbf{k}_x(\alpha) = \mathbf{k}_z(\alpha), \quad (65a)$$

$$\frac{d}{d\alpha} \mathbf{k}_y(\alpha) = \mathbf{0}, \quad (65b)$$

$$\frac{d}{d\alpha} \mathbf{k}_z(\alpha) = -\mathbf{k}_x(\alpha). \quad (65c)$$

Let θ ($\bar{\theta}$) be the angle between \mathbf{r}_P and \mathbf{r}_C , then

$$\sin \theta = \frac{x_{R,C}(\alpha)}{R}, \quad \cos \theta = \frac{z_{R,C}(\alpha)}{R}, \quad (66a)$$

$$\sin \bar{\theta} = \frac{\bar{x}_{R,C}(\alpha)}{R}, \quad \cos \bar{\theta} = \frac{\bar{z}_{R,C}(\alpha)}{R} \quad (66b)$$

and the tangent and normal vectors at C are

$$\mathbf{t}(\alpha) = \frac{z_{R,C}(\alpha)}{R} \mathbf{k}_x(\alpha) - \frac{x_{R,C}(\alpha)}{R} \mathbf{k}_z(\alpha), \quad (67a)$$

$$\mathbf{n}(\alpha) = \frac{x_{R,C}(\alpha)}{R} \mathbf{k}_x(\alpha) + \frac{z_{R,C}(\alpha)}{R} \mathbf{k}_z(\alpha), \quad (67b)$$

$$\bar{\mathbf{t}}(\alpha) = \frac{\bar{z}_{R,C}(\alpha)}{R} \mathbf{k}_x(\alpha) - \frac{\bar{x}_{R,C}(\alpha)}{R} \mathbf{k}_z(\alpha), \quad (67c)$$

$$\bar{\mathbf{n}}(\alpha) = \frac{\bar{x}_{R,C}(\alpha)}{R} \mathbf{k}_x(\alpha) + \frac{\bar{z}_{R,C}(\alpha)}{R} \mathbf{k}_z(\alpha). \quad (67d)$$

Differentiation of the tangent vector \mathbf{t} ($\bar{\mathbf{t}}$) with respect to the arclength s (\bar{s}) yields the curvature $\kappa(\alpha)$ ($\bar{\kappa}(\alpha)$) of the boundary

$$\frac{d}{ds} \mathbf{t}(\alpha) = \frac{d}{d\alpha} \mathbf{t}(\alpha) \frac{d\alpha}{ds} = \kappa(\alpha) \mathbf{n}(\alpha), \quad (68a)$$

$$\frac{d}{d\bar{s}} \bar{\mathbf{t}}(\alpha) = \frac{d}{d\alpha} \bar{\mathbf{t}}(\alpha) \frac{d\alpha}{d\bar{s}} = \bar{\kappa}(\alpha) \bar{\mathbf{n}}(\alpha). \quad (68b)$$

The derivative of the tangent vector $\mathbf{t}(\alpha)$ ($\bar{\mathbf{t}}(\alpha)$) with respect to α in normal direction is

$$\mathbf{n}(\alpha) \cdot \frac{d}{d\alpha} \mathbf{t}(\alpha) = \frac{x_{R,C}(\alpha) (x_{R,C}(\alpha) + z'_{R,C}(\alpha)) + z_{R,C}(\alpha) (z_{R,C}(\alpha) - x'_{R,C}(\alpha))}{R^2}, \quad (69a)$$

$$\bar{\mathbf{n}}(\alpha) \cdot \frac{d}{d\alpha} \bar{\mathbf{t}}(\alpha) = \frac{\bar{x}_{R,C}(\alpha) (\bar{x}_{R,C}(\alpha) + \bar{z}'_{R,C}(\alpha)) + \bar{z}_{R,C}(\alpha) (\bar{z}_{R,C}(\alpha) - \bar{x}'_{R,C}(\alpha))}{R^2} \quad (69b)$$

and the derivative of the arclength s (\bar{s}) with respect to α is equal to the change of the position of C in tangential direction

$$\frac{ds}{d\alpha} = \mathbf{t}(\alpha) \cdot \frac{d}{d\alpha} \mathbf{r}_{R,PC}(\alpha) = \frac{z_{R,C}(\alpha) (x'_{R,PC}(\alpha) - z_{R,PC}(\alpha)) - x_{R,C}(\alpha) (z'_{R,PC}(\alpha) + x_{R,PC}(\alpha))}{R}, \quad (70a)$$

$$\frac{d\bar{s}}{d\alpha} = \bar{\mathbf{t}}(\alpha) \cdot \frac{d}{d\alpha} \bar{\mathbf{r}}_{R,PC}(\alpha) = \frac{\bar{z}_{R,C}(\alpha) (\bar{x}'_{R,PC}(\alpha) - \bar{z}_{R,PC}(\alpha)) - \bar{x}_{R,C}(\alpha) (\bar{z}'_{R,PC}(\alpha) + \bar{x}_{R,PC}(\alpha))}{R} \quad (70b)$$

which yields the curvature

$$\kappa(\alpha) = \frac{x_{R,C}(\alpha) (x_{R,C}(\alpha) + z'_{R,C}(\alpha)) + z_{R,C}(\alpha) (z_{R,C}(\alpha) - x'_{R,C}(\alpha))}{R (z_{R,C}(\alpha) (x'_{R,PC}(\alpha) - z_{R,PC}(\alpha)) - x_{R,C}(\alpha) (z'_{R,PC}(\alpha) + x_{R,PC}(\alpha)))}, \quad (71a)$$

$$\bar{\kappa}(\alpha) = \frac{\bar{x}_{R,C}(\alpha) (\bar{x}_{R,C}(\alpha) + \bar{z}'_{R,C}(\alpha)) + \bar{z}_{R,C}(\alpha) (\bar{z}_{R,C}(\alpha) - \bar{x}'_{R,C}(\alpha))}{R (\bar{z}_{R,C}(\alpha) (\bar{x}'_{R,PC}(\alpha) - \bar{z}_{R,PC}(\alpha)) - \bar{x}_{R,C}(\alpha) (\bar{z}'_{R,PC}(\alpha) + \bar{x}_{R,PC}(\alpha)))}. \quad (71b)$$

The assumed uniqueness of C follows from two conditions: the curvature of the circle is always smaller than that of the body

$$R\kappa(\alpha) = \frac{x_{R,C}(\alpha) (x_{R,C}(\alpha) + z'_{R,C}(\alpha)) + z_{R,C}(\alpha) (z_{R,C}(\alpha) - x'_{R,C}(\alpha))}{z_{R,C}(\alpha) (x'_{R,PC}(\alpha) - z_{R,PC}(\alpha)) - x_{R,C}(\alpha) (z'_{R,PC}(\alpha) + x_{R,PC}(\alpha))} > -1, \quad (72a)$$

$$R\bar{\kappa}(\alpha) = \frac{\bar{x}_{R,C}(\alpha) (\bar{x}_{R,C}(\alpha) + \bar{z}'_{R,C}(\alpha)) + \bar{z}_{R,C}(\alpha) (\bar{z}_{R,C}(\alpha) - \bar{x}'_{R,C}(\alpha))}{\bar{z}_{R,C}(\alpha) (\bar{x}'_{R,PC}(\alpha) - \bar{z}_{R,PC}(\alpha)) - \bar{x}_{R,C}(\alpha) (\bar{z}'_{R,PC}(\alpha) + \bar{x}_{R,PC}(\alpha))} > -1. \quad (72b)$$

and the position of C on the boundary increases monotonically

$$\frac{d}{d\alpha} \varphi(\alpha) = 1 + \frac{x'_{R,PC}(\alpha) z_{R,PC}(\alpha) - x_{R,PC}(\alpha) z'_{R,PC}(\alpha)}{x_{R,PC}^2(\alpha) + z_{R,PC}^2(\alpha)} > 0, \quad (73a)$$

$$\frac{d}{d\alpha} \bar{\varphi}(\alpha) = 1 + \frac{\bar{x}'_{R,PC}(\alpha) \bar{z}_{R,PC}(\alpha) - \bar{x}_{R,PC}(\alpha) \bar{z}'_{R,PC}(\alpha)}{\bar{x}_{R,PC}^2(\alpha) + \bar{z}_{R,PC}^2(\alpha)} > 0. \quad (73b)$$

The almost convex case contains the contact problem between the body and a straight line from Sect. 4 as borderline case for the limit $R \rightarrow \infty$. Because

$$\lim_{R \rightarrow \infty} g_{R,P}(\alpha) \rightarrow \infty$$

a transformation to

$$\tilde{g}_{R,P}(\alpha) = g_{R,P}(\alpha) - R \quad (74)$$

is required to treat this case. The definition of $\tilde{g}_{R,P}(\alpha)$ is equal to the definition of $f_P(\alpha)$ in Sect. 4: both describe the

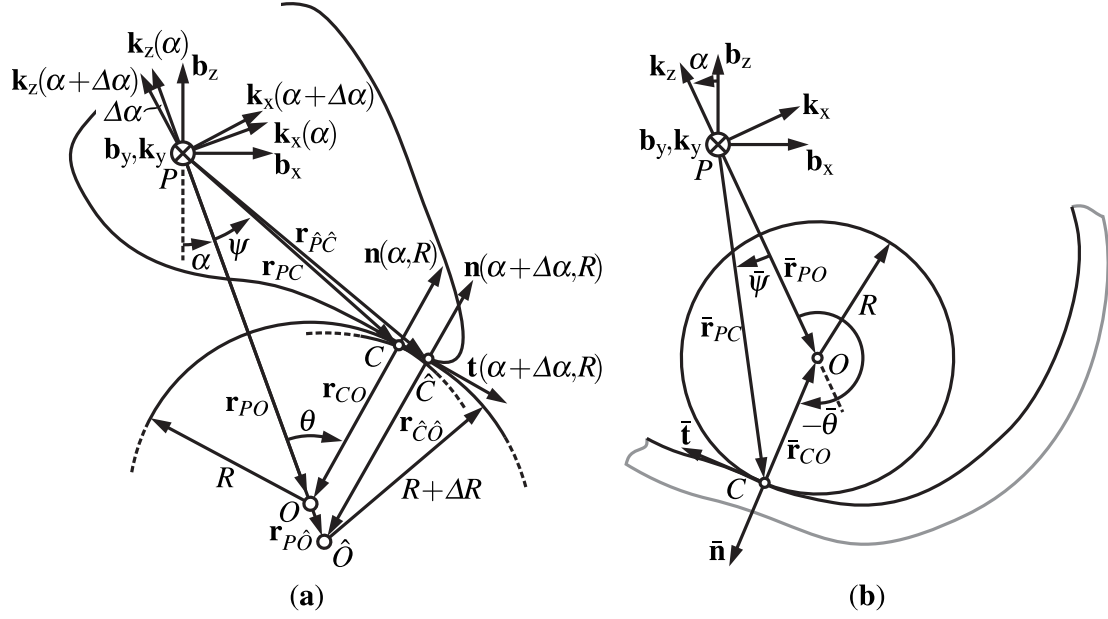


Figure 5: Boundary of (a) the almost convex body, and (b) the almost concave body in polar coordinates (observed in the body-fixed frame \mathcal{B}). The tangent and normal vectors at C are \mathbf{t} , \mathbf{n} and $\hat{\mathbf{t}}$, $\hat{\mathbf{n}}$, respectively. (a) displays the contact between the almost convex body and two circles with radii R and $R + \Delta R$, respectively, for the same angle α

minimum distance from P to the circle or line, respectively. Substitution of Eq. (74) and evaluation of the limit yields

$$z_{\infty,PC}(\alpha) = \lim_{R \rightarrow \infty} z_{R,PC}(\alpha) = \tilde{g}_{\infty,P}(\alpha), \quad (75a)$$

$$x_{\infty,PC}(\alpha) = \lim_{R \rightarrow \infty} x_{R,PC}(\alpha) = \tilde{g}'_{\infty,P}(\alpha), \quad (75b)$$

$$\begin{aligned} \lim_{R \rightarrow \infty} \kappa(\alpha) &= \left(z_{\infty,PC}(\alpha) + x'_{\infty,PC}(\alpha) \right)^{-1} \\ &= \left(\tilde{g}''_{\infty,P}(\alpha) + \tilde{g}_{\infty,P}(\alpha) \right)^{-1} \end{aligned} \quad (75c)$$

for Eqs. (55a), (55b) and (71a). These expressions are equal to Eqs. (19), (23) and (37) from Sect. 4. Furthermore, the borderline case for the limit $R \rightarrow 0$

$$z_{0,PC}(\alpha) = \lim_{R \rightarrow 0} z_{R,PC}(\alpha) = g_{0,P}(\alpha), \quad (76a)$$

$$x_{0,PC}(\alpha) = \lim_{R \rightarrow 0} x_{R,PC}(\alpha) = 0, \quad (76b)$$

$$\begin{aligned} \lim_{R \rightarrow 0} \kappa(\alpha) &= \lim_{R \rightarrow 0} \frac{\sqrt{1 - \left(\frac{x_{R,PC}(\alpha)}{R} \right)^2} - \frac{x'_{R,PC}(\alpha)}{R}}{\left(z_{R,PC}(\alpha) + x'_{R,PC}(\alpha) \right)} \\ &= \frac{g_{0,P}^2(\alpha) + 2g'_{0,P}{}^2(\alpha) - g''_{0,P}(\alpha)}{\left(g_{0,P}^2(\alpha) + g'_{0,P}{}^2(\alpha) \right)^{\frac{3}{2}}}, \end{aligned} \quad (76c)$$

where $g_{0,P}(\alpha) = \tilde{g}_{0,P}(\alpha)$, is an explicit parameterization of the body's boundary in polar coordinates with angle α and radius $g_{0,P}(\alpha)$. These observations motivate the investigation of whether there is an explicit transformation of $g_{R,P}(\alpha)$ from one circle radius R to another. An implicit transformation from any radius to $R \rightarrow 0$ is already given by Eqs. (57) and (59).

One approach for the explicit transformation of $g_{R,P}(\alpha) = g_P(\alpha, R)$ from one circle radius R to another is to derive a partial differential equation (PDE) in R and α and then examine if there are analytical solutions of the arising initial

value problem. Only the almost convex case is treated below; the procedure is analogous for the almost concave case. The PDE follows from the geometry in Fig. 5a which displays the contact between the body and the original circle with radius R , origin O and contact point C , and with another circle with radius $R + \Delta R$, origin \hat{O} and contact point \hat{C} for the same angle α . The position of \hat{O} in the body-fixed frame \mathcal{B} is

$$\mathbf{r}_{P\hat{O}} = -g_P(\alpha, R + \Delta R) \mathbf{k}_z(\alpha), \quad (77)$$

but also

$$\mathbf{r}_{P\hat{O}} = \mathbf{r}_{PC} + \mathbf{r}_{\hat{C}\hat{O}}. \quad (78)$$

The position of \hat{C} is equal to the contact point of the original circle with radius R for the angle $\alpha + \Delta\alpha$

$$\mathbf{r}_{PC} = x_{PC}(\alpha + \Delta\alpha, R) \mathbf{k}_x(\alpha + \Delta\alpha) + z_{PC}(\alpha + \Delta\alpha, R) \mathbf{k}_z(\alpha + \Delta\alpha). \quad (79)$$

The point \hat{O} is in direction of the normal vector at \hat{C} , therefore

$$\begin{aligned} \mathbf{r}_{\hat{C}\hat{O}} &= -(R + \Delta R) \mathbf{n}(\alpha + \Delta\alpha) \\ &= -(R + \Delta R) \frac{x_{PC}(\alpha + \Delta\alpha, R)}{R} \mathbf{k}_x(\alpha + \Delta\alpha) \\ &\quad - (R + \Delta R) \frac{\sqrt{R^2 - x_{PC}^2(\alpha + \Delta\alpha, R)}}{R} \mathbf{k}_z(\alpha + \Delta\alpha) \end{aligned} \quad (80)$$

and

$$\begin{aligned} \mathbf{r}_{P\hat{O}} &= -\Delta R \frac{x_{PC}(\alpha + \Delta\alpha, R)}{R} \mathbf{k}_x(\alpha + \Delta\alpha) \\ &\quad - \left(z_{PC}(\alpha + \Delta\alpha, R) + (R + \Delta R) \frac{\sqrt{R^2 - x_{PC}^2(\alpha + \Delta\alpha, R)}}{R} \right) \mathbf{k}_z(\alpha + \Delta\alpha). \end{aligned} \quad (81)$$

The goal is to derive a differential equation with respect to R and α which means the limits $\Delta R \rightarrow 0$ and $\Delta\alpha \rightarrow 0$ will be evaluated below. Therefore, the linearization of Eq. (81) is admissible and a comparison with the coefficient of Eq. (77) yields

$$\Delta\alpha = \frac{x_{PC}(\alpha, R)}{R(-z_{PC}(\alpha, R) + \sqrt{R^2 - x_{PC}^2(\alpha, R)})} \Delta R, \quad (82)$$

$$g_P(\alpha, R + \Delta R) = g_P(\alpha, R) + \sqrt{1 - \left(\frac{x_{PC}(\alpha, R)}{R}\right)^2} \Delta R. \quad (83)$$

The desired differential equation follows from Eq. (83) for the limit

$$\lim_{\Delta R \rightarrow 0} \frac{g_P(\alpha, R + \Delta R) - g_P(\alpha, R)}{\Delta R} = \partial_R g_P(\alpha, R) = \frac{g_P(\alpha, R)}{\sqrt{(g_P(\alpha, R))^2 + (\partial_\alpha g_P(\alpha, R))^2}} \quad (84)$$

(the shorthand $\partial_R = \frac{\partial}{\partial R}$ is used for partial derivatives). Unfortunately, we failed to find an explicit analytic solution $g_P(\alpha, R_1)$ for a general initial condition $g_P(\alpha, R_0)$, cf. Appendix A. Therefore, this approach does not yield the desired explicit transformation.

6. Examples

The results from Sect. 4 and 5 are applied to two example applications: a simple model of a rigid foot rolling on flat ground in Sect. 6.1 and a roller tappet in contact with a camshaft in Sect. 6.2.

6.1. Rigid foot on flat ground

A simple example for the contact of a convex rigid body with a straight line is motivated by two-dimensional models for human walking and running. Although human feet are complex structures which consist of several bones, tendons, muscles and other tissue, a common model simplification in biomechanics is the rigid body approximation, so called rollover shapes [14]. This approximation does not model the feet's internal structure, however, it captures their influence on the whole body dynamics and can be used for contact detection and force calculations. The goal of this example is to derive the equations of motion for a single detached foot (no connection to the remainder of the body) which is rolling on the ground. The contact forces are derived to check the rolling condition (no slipping).

For the sake of simplicity, we do without fitting to experimental data and use the simple ansatz

$$f_P(\alpha) = R \left(1 + \frac{9}{10} \cos\left(\alpha - \frac{\pi}{5}\right) + \frac{1}{6} \sin\left(2\left(\alpha - \frac{\pi}{5}\right)\right) + \frac{1}{15} \sin\left(3\left(\alpha - \frac{\pi}{5}\right)\right) \right) \quad (85)$$

$$\alpha \in \left[-\frac{\pi}{2}, \frac{\pi}{2} \right],$$

to generate the shape in Fig. 6a. The coefficients have been tuned to satisfy condition of positive curvature via Eq. (37). The reference point P is representing the assumed center of mass (mass m , inertia J_P) and the limits for α restrict the rolling motion to the foot's sole. The kinematics of the ankle joint A can be derived by Eqs. (38) – (42) with \mathbf{r}_{PA} and α_{PA} via Fig. 6a. There are no external forces except for gravity (g). The equation of motion can be derived from the kinetic and potential energy

$$\begin{aligned} T &= \frac{1}{2} m (\dot{x}_P^2 + \dot{z}_P^2) + \frac{1}{2} J_P \dot{\alpha}^2 \\ &= \frac{1}{2} (m x_P'^2(\alpha) + m z_P'^2(\alpha) + J_P) \dot{\alpha}^2 \\ &= \frac{1}{2} (m f_P^2(\alpha) + m f_P'^2(\alpha) + J_P) \dot{\alpha}^2, \end{aligned} \quad (86a)$$

$$\begin{aligned} V &= m g z_P(\alpha) \\ &= m g f_P(\alpha) \end{aligned} \quad (86b)$$

using Lagrange equations

$$\begin{aligned} \frac{d}{dt} \frac{\partial}{\partial \dot{\alpha}} (T - V) - \frac{\partial}{\partial \alpha} (T - V) &= 0 \\ \Rightarrow (m f_P^2(\alpha) + m f_P'^2(\alpha) + J_P) \ddot{\alpha} + m f_P'(\alpha) (f_P(\alpha) + f_P''(\alpha)) \dot{\alpha}^2 + m g f_P'(\alpha) &= 0. \end{aligned} \quad (87)$$

The forces at the contact point C are

$$F_{C,x} = m \ddot{x}_P = m (f_P(\alpha) \ddot{\alpha} + f_P'(\alpha) \dot{\alpha}^2), \quad (88a)$$

$$F_{C,z} = m \ddot{z}_P + m g = m (f_P'(\alpha) \ddot{\alpha} + f_P''(\alpha) \dot{\alpha}^2 + g) \quad (88b)$$

from the balance of forces via Fig. 6b. The equation of motion (87) can be solved numerically. The rolling conditions are

$$0 \leq F_{C,z}, \quad (89a)$$

$$|F_{C,x}| \leq \mu_0 |F_{C,z}| \quad (89b)$$

with the coefficient of static friction μ_0 .

6.2. Camshaft and roller tappet

The combination of a camshaft and roller tappets is a frequently used mechanism for the control of valves in internal combustion engines. This contact is typically lubricated which means the contact forces follow from the

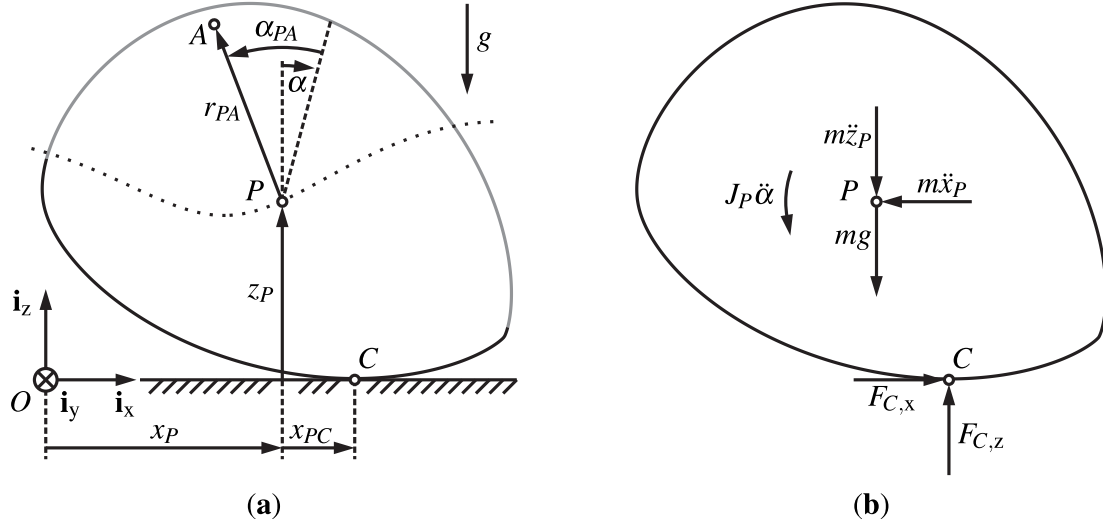


Figure 6: (a) Model of a rigid foot rolling on flat ground, and (b) corresponding free body diagram. The foot's sole is illustrated in black, the remaining boundary in gray. The dotted line is the trajectory of P

elastohydrodynamic lubrication theory [15]. However, this level of complexity is beyond the scope of this paper, which is why the dissipative contact model which was proposed by Hunt and Crossley [16] is used in the treatment below.

The system is displayed in Fig. 7a. The roller tappet is guided in vertical \mathbf{k}_z -direction and preloaded by a linear spring with stiffness c and relaxed position z_0 . The center of mass of the roller tappet (total mass m) is assumed to be in its center M . The roller's radius is R and the rotational inertia with respect to M is J_M . The camshaft is rotating around the origin P . Its orientation with respect to the inertial system \mathcal{K} is $\alpha(t) = \dot{\alpha}_0 t$ with the constant angular velocity $\dot{\alpha} = \dot{\alpha}_0$. The translation and rotation of the roller are described by the position z_M and its angle ϕ . The problem follows from the description in Sect. 5 by a rotation with the angle ϕ and a shift of the origin from M to P . For the sake of simplicity gravity is neglected.

The almost convex cam geometry in Fig. 7a is described by the piecewise function

$$g_{R,P}(\alpha) = \begin{cases} 2R + \left(\frac{1}{3}\left(\alpha - \frac{2}{3}\pi\right)^3\left(\frac{4}{3}\pi - \alpha\right)^4\right)R & \text{if } \frac{2}{3}\pi < \alpha < \frac{4}{3}\pi \\ 2R & \text{otherwise} \end{cases} \quad (90)$$

with $g_{R,P}(\alpha) \in C^2$ for $\alpha \in \mathbb{S}$. Because $g_{R,P}(\alpha)$ is twice continuously differentiable, the cam's curvature is continuous which is a necessary requirement for the contact force model. There is a concave section of the cam's boundary with negative curvature, however, there is always a unique contact point with the roller. The positions of the potential contact points C on the cam's boundary and C' on the roller follow from

$$\mathbf{r}_C = x_{R,PC}(\alpha) \mathbf{k}_x + z_{R,PC}(\alpha) \mathbf{k}_z, \quad (91)$$

$$\mathbf{r}_{C'} = \mathbf{r}_M + \mathbf{r}_{MC'}, \quad (92)$$

$$\mathbf{r}_{MC'} = x_{R,C}(\alpha) \mathbf{k}_x + z_{R,C}(\alpha) \mathbf{k}_z \quad (93)$$

with the roller's position

$$\mathbf{r}_M = z_M \mathbf{k}_z \quad (94)$$

and the contact force is

$$\begin{aligned}\mathbf{F}_C &= F_{C,t} \mathbf{t} + F_{C,n} \mathbf{n} \\ &= F_{C,x} \mathbf{k}_x + F_{C,z} \mathbf{k}_z.\end{aligned}\quad (100)$$

The dissipative force contact model which was proposed by Hunt and Crossley [16] assumes small deformations of the bodies' boundaries at the contact point which are an extension of the Hertz contact theory [12]. The deformation is calculated from the penetration of the original (rigid) geometries

$$\delta = (\mathbf{r}_{C'} - \mathbf{r}_C) \cdot \mathbf{n} \quad (101)$$

and the corresponding relative velocity in normal and tangential direction

$$\dot{\delta} = (\mathbf{v}_{C'} - \mathbf{v}_C) \cdot \mathbf{n}, \quad (102a)$$

$$\mathbf{v}_{\text{rel},t} = (\mathbf{v}_{C'} - \mathbf{v}_C) \cdot \mathbf{t}. \quad (102b)$$

This results (cf. [12, Eqs. (18)–(30)]) in a force law for the normal component

$$F_{C,n} = \begin{cases} K \delta^{3/2} \left[1 + \frac{3(1-c_r)}{2} \frac{\dot{\delta}}{\delta^{(-)}} \right] & \text{for } \delta \geq 0 \\ 0 & \text{for } \delta < 0 \end{cases} \quad (103)$$

with

$$K = \frac{4}{3} \left(\frac{1-\nu_1^2}{E_1} + \frac{1-\nu_2^2}{E_2} \right)^{-1} \sqrt{\left(\frac{1}{R} + \kappa(\alpha) \right)^{-1}}, \quad (104)$$

where E_1, E_2 are the bodies' Young's moduli, ν_1, ν_2 are their Poisson's ratios, c_r denotes the coefficient of restitution and $\delta^{(-)}$ is the initial impact velocity. The bodies are separated if $\delta < 0$ and there is no interaction at the potential contact points. The tangential component of the contact force is modeled via

$$F_{C,t} = \mu \tanh\left(\frac{\mathbf{v}_{\text{rel},t}}{k}\right) F_{C,n} \quad (105)$$

which is a regularization of Coulomb's friction law with the coefficient of sliding friction μ . For large values of the regularization parameter k the hyperbolic tangent approximates the sign function

$$\lim_{k \rightarrow \infty} \tanh\left(\frac{\mathbf{v}_{\text{rel},t}}{k}\right) = \text{sign}(\mathbf{v}_{\text{rel},t}).$$

This model for the contact force does not consider rolling friction due to the fact that the material contact points of the rotating bodies change constantly. Furthermore, due to the exponent in Eq. (103) a point contact is considered, although a line contact may seem more plausible for a planer model. However, the purpose of this example is to demonstrate the simple implementation of the presented approach and its combination with more complex descriptions of the interaction force at the contact points.

The system's equations of motion

$$m \ddot{z}_M = c(z_0 - z_M) - F_{C,z}, \quad (106a)$$

$$J_M \ddot{\phi} = R F_{C,t} \quad (106b)$$

are solved numerically using *Matlab* using the following parameters: $E_1 = E_2 = 2.1 \cdot 10^{11}$ N/m², $\nu_1 = \nu_2 = 0.3$, $c_r = 0.6$, $\mu = 0.6$, $k = 100$ m/s, $c = 200$ N/m, $z_0 = 0$ m, $R = 0.01$ m, $m = 0.025$ kg, $J_M = 1.25 \cdot 10^{-6}$ kg m² and $\dot{\alpha}_0 = 100$ rad/s. This choice of parameters causes the roller to lift-off during every revolution of the cam. It is then pushed back by the spring until it collides with the roller. The solution for z_M and δ are displayed in Fig. 8. A video of the solution as well as the *Matlab*-implementation used for the simulation are provided as electronic supplementary to this paper.

Both examples highlight the simple application of the presented approach in mechanical models of planar systems.

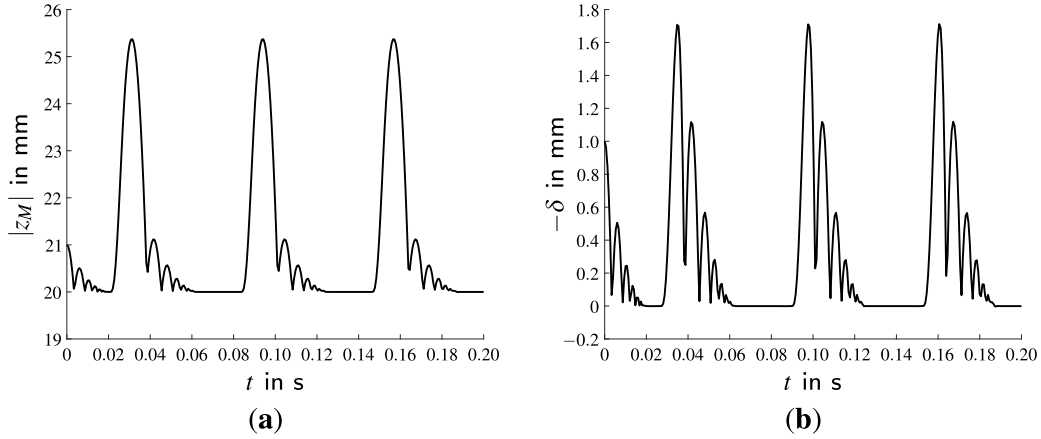


Figure 8: (a) Distance between P and M , and (b) gap (negative penetration $-\delta$) for the cam-follower system with lift-off of the roller

7. Conclusion

In this paper a solution for two-dimensional contact detection problems between a body with complex geometry and a straight line or a circle is presented. Explicit formulas for the position of the (potential) contact point C which depend on the body's orientation α relative to the counterpart are derived. An arbitrary body-fixed reference point P is chosen and its distance from the line or the circle's center is parameterized as an explicit function of α assuming there is contact. The position of C relative to P as well as the corresponding curvature follow from the special case of a rolling contact as explicit functions of α . The presented procedure requires uniqueness of C for all angles α and piecewise smoothness of the body's boundary. The smoothness of the resulting parameterization depends only on the smoothness of the generating functions which have to be derived once. The contact detection problem between a body and a circle has two solutions which correspond to the almost convex and the almost concave case, respectively (cf. Sect. 5). For the limit of an infinite circle radius the expressions for the almost convex case are equal to the ones for the contact with a straight line.

The developed method is applied to two examples in Sect. 6: the biomechanical model of a rigid foot rolling on flat ground and the technical system of a camshaft actuating a roller tappet. In the first example, a Fourier series with three harmonics is used to parameterize the rigid foot. Its equation of motion can be derived as an ordinary differential equation for the angle α . In the second example, the cam geometry is parameterized by a piecewise function with continuous curvature. The interaction is described by a dissipative contact force model (Hunt and Crossley [16]). A numerical solution which includes separation of the roller from the cam and subsequent impacts is presented. Both examples highlight the easy application of the derived relationships to specific systems which involve the discussed contact detection problems. They can also be implemented as special contact elements in multibody software environments, e.g. modelica [17]. The presented procedure can be generalized to three-dimensional contact detection problems. A solution for the contact between a convex body and a planar counterpart will be provided shortly.

Appendix A. Analytical solution of initial value problem for PDE (84)

Stating PDE (84) from Sect. 5 in the conventional analysis notation gives

$$\partial_y u(x, y) = \frac{u(x, y)}{\sqrt{u^2(x, y) + (\partial_x u(x, y))^2}}, \quad (\text{A.1})$$

$u : \mathbb{S} \times \mathbb{R}_{0+} \rightarrow \mathbb{R}_+$ which is a nonlinear PDE of the first order. Amongst the many methods for the analytical solution of PDEs, there are two which follow a strict procedure⁴: separation of variables and the calculation of a characteristic strip. Equation (A.1) can indeed be solved by the separation ansatz

$$u(x, y) = X(x) \cdot Y(y) \quad (\text{A.2})$$

which yields

$$\begin{aligned} X(x)Y'(y) &= \frac{X(x)Y(y)}{\sqrt{X(x)^2Y^2(y) + X'^2(x)Y^2(y)}} \\ \Leftrightarrow \text{sign}(Y(y)) Y'(y) &= \frac{1}{\sqrt{X^2(x) + X'^2(x)}} = k \end{aligned} \quad (\text{A.3})$$

with $k \in \mathbb{R}_+$. The only solution is

$$X(x) = \frac{\cos(x + c_1)}{k}, \quad c_1 \in \mathbb{S}, \quad (\text{A.4a})$$

$$Y(y) = k(y + c_2), \quad c_2 \in \mathbb{R}, \quad (\text{A.4b})$$

$$u(x, y) = (y + c_2) \cos(x + c_1). \quad (\text{A.4c})$$

However, this solution cannot be adjusted to arbitrary initial conditions $u(x, y_0) = u_0(x)$ and, furthermore, $u \notin \mathbb{R}_+$ due to the alternating sign of the cosine rendering it useless for the desired application.

Therefore, the calculation of a characteristic strip is investigated, cf. [18]. Equation (A.1) equals

$$0 = q \sqrt{z^2 + p^2} - z = F(x, y, z, p, q) \quad (\text{A.5})$$

with

$$z = u(x, y),$$

$$p = \partial_x u(x, y),$$

$$q = \partial_y u(x, y).$$

This results in a set of ordinary differential equations in the new variable t

$$x'(t) = \partial_p F(x, y, z, p, q) = \frac{q^2(t)p(t)}{z(t)}, \quad (\text{A.6a})$$

$$y'(t) = \partial_q F(x, y, z, p, q) = \frac{z(t)}{q(t)}, \quad (\text{A.6b})$$

$$z'(t) = p \partial_p F(x, y, z, p, q) + q \partial_q F(x, y, z, p, q) = z(t) (2 - q^2(t)), \quad (\text{A.6c})$$

$$p'(t) = -\partial_x F(x, y, z, p, q) - p \partial_z F(x, y, z, p, q) = p(t) (1 - q^2(t)), \quad (\text{A.6d})$$

$$q'(t) = -\partial_y F(x, y, z, p, q) - q \partial_z F(x, y, z, p, q) = q(t) (1 - q^2(t)) \quad (\text{A.6e})$$

⁴Other methods also follow strict procedures. However, these procedures include steps like finding a suitable transformation (e.g. Bäcklund transformation) which is not trivial even if it exists.

with the recursive solution

$$q(s, t) = \frac{c_1(s)}{\sqrt{c_1^2(s) + e^{-2t}}}, \quad (\text{A.7a})$$

$$p(s, t) = \frac{c_2(s)}{\sqrt{c_1^2(s) + e^{-2t}}}, \quad (\text{A.7b})$$

$$z(s, t) = \frac{c_1(s)}{\sqrt{c_1^2(s) + e^{-2t}}} c_3(s) e^t, \quad (\text{A.7c})$$

$$y(s, t) = c_3(s) e^t + c_4(s), \quad (\text{A.7d})$$

$$x(s, t) = \frac{c_2(s)}{c_3(s)} \arctan(c_1(s) e^t) + c_5(s). \quad (\text{A.7e})$$

The unknowns $c_i(s)$, $i = 1, \dots, 5$ are determined by the initial conditions for $t = 0$:

$$c_1(s) = \frac{q_0(s)}{\sqrt{1 - q_0^2(s)}}, \quad (\text{A.8a})$$

$$c_2(s) = \frac{p_0(s)}{\sqrt{1 - q_0^2(s)}}, \quad (\text{A.8b})$$

$$c_3(s) = \frac{z_0(s)}{q_0(s)}, \quad (\text{A.8c})$$

$$c_4(s) = y_0(s) - \frac{z_0(s)}{q_0(s)}, \quad (\text{A.8d})$$

$$c_5(s) = x_0(s) - \frac{p_0(s)}{z_0(s)} \frac{q_0(s)}{\sqrt{1 - q_0^2(s)}} \arctan\left(\frac{q_0(s)}{\sqrt{1 - q_0^2(s)}}\right). \quad (\text{A.8e})$$

One possibility to transform the initial condition $u(x, y_0) = u_0(x)$ to the coordinates s, t is

$$x(s, t = 0) = f(s) = s, \quad (\text{A.9a})$$

$$y(s, t = 0) = g(s) = y_0, \quad (\text{A.9b})$$

$$z(s, t = 0) = h(s) = u_0(s), \quad (\text{A.9c})$$

$$p(s, t = 0) = \phi(s), \quad (\text{A.9d})$$

$$q(s, t = 0) = \psi(s) \quad (\text{A.9e})$$

where $\phi(s)$ and $\psi(s)$ must be such that

$$h'(s_0) = \phi(s_0)f'(s_0) + \psi(s_0)g'(s_0), \quad (\text{A.10a})$$

$$0 = F(x_0, y_0, z_0, p_0, q_0), \quad (\text{A.10b})$$

$$0 \neq f'(s_0)F_q(x_0, y_0, z_0, p_0, q_0) - g'(s_0)F_p(x_0, y_0, z_0, p_0, q_0). \quad (\text{A.10c})$$

Equation (A.10a) implies

$$\phi(s) = u'_0(s) \quad (\text{A.11})$$

which in turn yields

$$\psi(s) = \frac{u_0(s)}{\sqrt{(u_0(s))^2 + (u'_0(s))^2}}. \quad (\text{A.12})$$

Equations (A.11) and (A.12) also satisfy Eq. (A.10c) because $z_0 \in \mathbb{R}_+$. Adjusting the general solution to these initial conditions results in

$$x(s, t) = s + \arctan\left(\frac{u_0(s)}{u'_0(s)} e^t\right) - \arctan\left(\frac{u_0(s)}{u'_0(s)}\right), \quad (\text{A.13a})$$

$$y(s, t) = y_0 + (e^t - 1) \sqrt{(u_0(s))^2 + (u'_0(s))^2}, \quad (\text{A.13b})$$

$$z(s, t) = \frac{\sqrt{(u_0(s))^2 + (u'_0(s))^2}}{\sqrt{(u_0(s))^2 + e^{-2t}(u'_0(s))^2}} u_0(s) e^t. \quad (\text{A.13c})$$

The general solution $z(x, y) = z(x(s, t), y(s, t))$ thus obtained is still implicit in x and y . To finish the characteristic strip method, explicit expressions $s(x, y)$ and $t(x, y)$ are required. However, there is no explicit solution of Eqs. (A.13) for s and t which means that this approach does not yield an explicit solution of PDE (A.1).

References

- [1] C. Wellmann, C. Lillie, P. Wriggers, A contact detection algorithm for superellipsoids based on the common-normal concept, *Eng. Comp.* 25 (5) (2008) 432–442. doi:10.1108/02644400810881374.
- [2] D. S. Lopes, R. R. Neptune, J. A. Ambrósio, M. T. Silva, A superellipsoid-plane model for simulating foot-ground contact during human gait, *Comput. Methods Biomec.* 19 (9) (2016) 954–963. doi:10.1080/10255842.2015.1081181.
- [3] X. Zheng, P. Palfy-Muhoray, Distance of closest approach of two arbitrary hard ellipses in two dimensions, *Phys. Rev. E* 75 (6) (2007) 061709. doi:10.1103/PhysRevE.75.061709.
- [4] P. Wriggers, *Computational Contact Mechanics*, 2nd Edition, Springer-Verlag Berlin Heidelberg, 2006. doi:10.1007/978-3-540-32609-0.
- [5] X. Zheng, W. Iglesias, P. Palfy-Muhoray, Distance of closest approach of two arbitrary hard ellipsoids, *Phys. Rev. E* 79 (5) (2009) 057702. doi:10.1103/PhysRevE.79.057702.
- [6] D. S. Lopes, M. T. Silva, J. A. Ambrósio, P. Flores, A mathematical framework for rigid contact detection between quadric and superquadric surfaces, *Multibody Syst. Dyn.* 24 (3) (2010) 255–280. doi:10.1007/s11044-010-9220-0.
- [7] A. A. Gonçalves, A. Bernardino, J. Jorge, D. S. Lopes, A benchmark study on accuracy-controlled distance calculation between superellipsoid and superovoid contact geometries, *Mech. Mach. Theory* 115 (2017) 77–96. doi:10.1016/j.mechmachtheory.2017.04.008.
- [8] E. Hairer, G. Wanner, *Solving Ordinary Differential Equations II*, 2nd Edition, Springer-Verlag, Berlin, 1996. doi:10.1007/978-3-642-05221-7.
- [9] K. L. Johnson, *Contact Mechanics*, Cambridge University Press, Cambridge, 1987.
- [10] L. X. Xu, A method for modelling contact between circular and non-circular shapes with variable radii of curvature and its application in planar mechanical systems, *Multibody Syst. Dyn.* 39 (3) (2017) 153–174. doi:10.1007/s11044-016-9549-0.
- [11] R. T. Faroukia, J. Manjunathaiah, S. Jeeb, Design of rational cam profiles with pythagorean-hodograph curves, *Mech. Mach. Theory* 33 (6) (1998) 669–682. doi:10.1016/S0094-114X(97)00099-2.
- [12] M. Machado, P. Moreira, P. Flores, H. M. Lankarani, Compliant contact force models in multibody dynamics: Evolution of the Hertz contact theory, *Mech. Mach. Theory* 53 (2012) 99–121. doi:10.1016/j.mechmachtheory.2012.02.010.
- [13] H. Hertz, Über die Berührung fester elastischer Körper, *Journal für die reine und angewandte Mathematik* 92 (1882) 156–171. doi:10.1515/crll.1882.92.156.
- [14] L. Ren, D. Howard, L. Ren, C. Nester, L. Tian, A generic analytical foot rollover model for predicting translational ankle kinematics in gait simulation studies, *J. Biomech.* 43 (2) (2010) 194–202. doi:10.1016/j.jbiomech.2009.09.027.
- [15] D. Dowson, G. R. Higginson, *Elasto-hydrodynamic lubrication*, SI Edition, Vol. 23 of International Series in Materials Science and Technology, Pergamon Press, Oxford, 1977.
- [16] K. H. Hunt, F. R. E. Crossley, Coefficient of Restitution Interpreted as Damping in Vibroimpact, *J. Appl. Mech.* 42 (2) (1975) 440–445. doi:10.1115/1.3423596.
- [17] P. Fritzson, V. Engelson, *Modelica — A unified object-oriented language for system modeling and simulation*, Springer, Berlin, 1998, pp. 67–90. doi:10.1007/BFb0054087.
- [18] F. John, *Partial Differential Equations*, 4th Edition, Vol. 1 of Applied Mathematical Sciences, Springer-Verlag New York, 1986, 54–93.